Micro-cogeneration versus conventional technologies: considering model uncertainties in assessing the energy benefits

Geoffrey Johnson[a], Ian Beausoleil-Morrison[b], Adam Wills[c]

[a] *Sustainable Building Energy Systems, Faculty of Engineering and Design, Carleton University, Ottawa, Canada, geoffreyjohnson@cmail.carleton.ca*
[b] *Sustainable Building Energy Systems, Faculty of Engineering and Design, Carleton University, Ottawa, Canada, Ian_Beausoleil-Morrison@carleton.ca*
[c] *Sustainable Building Energy Systems, Faculty of Engineering and Design, Carleton University, Ottawa, Canada, adamwills@cmail.carleton.ca*

Abstract

Fuel cells with nominal outputs of approximately 1 kW_{AC} are emerging as a prime-mover of a micro-cogeneration system potentially well-suited to compete, on an energy basis, with conventional methods for satisfying occupant electrical and thermal demands in a residential application. As the energy benefits of these systems can be incremental when compared to efficient conventional methods, it is especially important to consider the uncertainties of the models on which simulation results are based. However, researchers have yet to take this aspect into account.

This article makes a contribution by demonstrating how these model uncertainties may be propagated to the simulation results of a micro-cogeneration system for comparison to a reference scenario using a case study. This case study compares the energy performance of a fuel-cell based micro-cogeneration system serving only domestic hot water demands to an efficient reference scenario where the conventional methods for providing electrical and thermal demands are considered to be a central gas-fired combined-cycle plant and a condensing tankless water heater respectively. The simulation results demonstrated that if model uncertainties were ignored, it would have been possible to demonstrate that the considered micro-cogeneration system was more efficient than the reference scenario for average consumption levels of domestic hot water. However, when model uncertainties were considered the efficiency of the considered micro-cogeneration system could not reliably exceed that of the reference scenario by serving the domestic hot water needs of a single-family home.

Keywords: Residential buildings, Micro-cogeneration, Proton-exchange membrane fuel cell, Building performance simulation

---

Nomenclature

Symbol	Description
E	energy (J)
P	power (W)
ζ	efficiency
PI_{el}	electrical performance index
U_{95}	95% confidence interval
b	individual independent source of bias
B	total bias
σ	standard deviation
Z	z-score of normal distribution
p	probability
m_{CO_2-ref}	mass of CO_2 emissions (kg)
$GHGF$	greenhouse gas factor (kg m^{-3})
LHV	lower heating value of fuel (MJ m^{-3})
HHV	higher heating value of fuel (MJ m^{-3})
$V_{fuel-ref}$	volume of reference scenario fuel consumption (m^3)
Ψ	fraction of fuel-cell thermal output that is useful
q_{fc}	fuel-cell thermal output (W)
q_{loss}	standing loss of hot water storage tank (W)
T_{Tank}	temperature of hot water storage tank (^{o}C)
T_{fc-in}	temperature water at inlet of fuel-cell (^{o}C)
Δt	duration of simulation (s)

Subscript	Description
TWH	tankless water heater
DHW	domestic hot water
$el-t$	electrical transmission system
$el-d$	electrical distribution system
$el-ref$	reference scenario
$el-plant$	central electrical power plant
$fc-ac$	fuel-cell ac production
$fc-dc$	fuel-cell dc production
$fc-fuel$	fuel-cell fuel consumption
$fuel-TWH$	tankless water heater fuel consumption
$el-TWH$	tankless water heater electrical consumption
$el-aux$	auxiliary heater electrical consumption
$E_{el-cogen}$	net electrical production of cogeneration case plant network
E_{el-RS}	net electrical production of reference case plant network
$E_{fuel-cogen}$	fuel consumption of cogeneration case plant network
$E_{fuel-th-RS}$	fuel consumption of reference case plant network
$\zeta_{el-ref}-PI_{el}$	difference between reference scenario efficiency and micro-cogeneration electrical performance index

1. Introduction

Fuel cells with electrical outputs of approximately 1 kW are gaining interest as an efficient prime-mover of a micro-cogeneration system for a residential application in a single-family home. It was suggested in Annex 42 [1] that the performance of these systems should be compared to a reference scenario where occupant thermal and electrical demands are supplied by efficient conventional methods. Since then, there has been a European Commission decision to establish reference electrical and thermal efficiency values for this comparison [2] for its member states. Because the performance benefits of these systems compared to reference scenarios can be incremental [3], and comparison metrics can be very sensitive to small changes in efficiency values [4], it is especially important to consider the uncertainty margins of these comparison metrics.

Prior to when Johnson et al. [5] presented a model based on data with well-described uncertainties, it would not have been possible to propagate a model's uncertainties to the results from a simulation for an application similar to the one considered here. A model of a larger 2.8 kW solid-oxide fuel cell (SOFC) with well-described uncertainties was presented earlier [6] but is over-sized for this application.

There have been several simulation-based studies [7-10] that used the model presented by Johnson et al. [5], but none have taken into account the model's uncertainties in their results. There are also many recent examples of researchers [11-35] who have conducted simulations with a fuel cell in the range of outputs considered here using other models, but none with model uncertainties documented in as much detail as the model presented by Johnson et al. [5].

Notably, the model used by Canelli et al. [36] was calibrated with data originating from an earlier version of the apparatus used by Johnson et al. [5]. Canelli et al. [36] have cited a conference paper [37] as the origin of their data (as was also done by references [38, 39]) where the model uncertainties were not yet defined. However, it is not justifiable to use this model for this work when data with documented uncertainties from the same fuel cell exists and are available [5].

All widely available fuel cell models for building performance simulation were reviewed by Ham et al. [40] who determined that the model presented by Johnson et al. [5] was still the most accurate and concise. They provided new data for a PEMFC that is oversized (10 kW nominal electrical output) for the application under consideration in this work. They also fit a different model to the calibration data presented by Johnson et al. [5]. However, this new model is of limited validity for this work because it contains simplifications whose influences on the model's uncertainties were not described.

Aside from these models, there are several other studies with fuel cell data that deserve mentioning. References [41], [42] and [43] all provided data from a 1.5 kW SOFC whose electrical efficiency is 60% at rated conditions. Hody et al. [44] presented some more data describing the performance of several SOFCs and PEMFCs in the 1-4 kW output range at nominal operating conditions. References [45], [46], [47] and [48] provided some performance data from several 0.7 kW fuel cells. References [49] and [50] described field-trials where fuel cells at this 0.7 kW scale were demonstrated. In comparison with the performance of the fuel cell studied by Johnson et al. [5], the electrical efficiencies of these fuel cells appears to be superior. However, details describing the uncertainty of the performance data presented by these studies are unavailable so these models may not be used for this application.

1.1. Contributions

This article makes a contribution by developing a methodology where the uncertainty of component models is taken into account and then propagated to the results of simulations. For this methodology, the energy performance of a micro-cogeneration system is compared with a reference scenario where efficient conventional methods are used for providing occupant electrical and thermal demands. Therefore, estimating the uncertainties of the reference scenario is an aspect that also needs to be considered in this methodology.

This methodology is demonstrated in this article with a case study. In this case study, the energy performance of a 1 kW PEMFC in a residential application serving only domestic hot water (DHW) demands is compared to a reference scenario where a condensing tankless water heater (TWH) and a central gas-fired combined-cycle plant are used instead to provide occupant thermal and electrical demands. The reference scenario is appropriate for Ontario, Canada. This article expands upon the work of Johnson et al. [3].

In this article, first a description of this new methodology is provided. Following this, a more detailed description of the plant networks to be considered in this simulation-based case study to demonstrate this methodology is provided. Finally, the results of these simulations are interpreted using this new methodology before conclusions are drawn.

2. Methodology

2.1. Equivalent Electrical Performance Index Definition

An electrical performance index (PI_{el}) can be used [3] as a metric to compare the energy performance of a micro-cogeneration case with a reference scenario. The plant networks corresponding to the micro-cogeneration case and reference scenario to be considered as the case study considered in this article are illustrated later in Figure 1 in Section 3. The basic definition of PI_{el} is given in equation 1.

$$PI_{el} = \frac{E_{el-cogen} - E_{el-RS}}{E_{fuel-cogen} - E_{fuel-th-RS}} \quad (1)$$

Equation 1 considers that the equivalent electrical benefit of the thermal output of a micro-cogeneration system is that it displaces the fuel consumption of the conventional method in the reference scenario for providing occupant thermal demands. For this reason, the denominator of equation 1 is the net fuel consumption of the micro-cogeneration system ($E_{fuel-cogen}$) relative to the fuel consumption of the reference method for providing occupant thermal demands in the reference scenario ($E_{fuel-th-RS}$) that has been displaced.

Equation 1 also considers that there may be some additional benefit (or penalty) related to the displaced electrical consumption of the conventional method for providing thermal demands. For example, the electrical consumption of a reference heater whose thermal output is displaced by the thermal output of a micro-cogeneration system. Therefore, the numerator in equation 1 is the difference between the net electrical production of the micro-cogeneration case ($E_{el-cogen}$) relative to the net electrical production of reference scenario (E_{el-RS}). Note that net electrical production is defined for the micro-cogeneration case as the difference between the micro-cogeneration system's electrical production and the electrical consumption of the other plant network components. In comparison, the net electrical production of the reference scenario is defined entirely as the negative value of the electrical consumption of the other plant network components.

It is also noteworthy that equation 1 is the electrical analog of the equivalent thermal coefficient of performance used by Staffell [4]. The PI_{el} in equation 8 is directly comparable with the electrical efficiency of the conventional method for providing electrical demands in the reference scenario (ζ_{el-ref}) described in Section 3.4. If the PI_{el} of the micro-cogneration case exceeds the ζ_{el-ref} of the reference scenario, then fuel is used more efficiently in the micro-cogeneration case.

2.2. p-Value Definition

All of the terms on the right side of equation 1 have uncertainty margins associated with them, therefore, the PI_{el} does as well. These margins can be used to determine the probability that the reference scenario efficiency exceeds the PEMFC micro-cogeneration case ($p(\zeta_{el-ref} > PI_{el})$). This is termed the p-Value. If this p-Value is small then it is likely that the micro-cogeneration case is more efficient than the reference scenario. For this research, if the p-Value is less than 0.05 it will be assumed that the micro-cogeneration case is more efficient.

Equation 2 essentially states that to determine the p-Value it is equivalent to determine the probability that the difference between ζ_{el-ref} relative to PI_{el} is greater than zero.

$$p(\zeta_{el-ref} > PI_{el}) = p(\zeta_{el-ref} - PI_{el} > 0) \tag{2}$$

This probability can be assessed using the Standard Normal Distribution with corresponding Z statistics according to equation 3.

$$p(\zeta_{el-ref} - PI_{el} > 0) = p(Z_{\zeta_{el-ref}-PI_{el}} > 0) \quad (3)$$

Where $Z_{\zeta_{el-ref}-PI_{el}}$ can be found from equation 4.

$$Z_{\zeta_{el-ref}-PI_{el}} = \frac{\zeta_{el-ref} - PI_{el}}{\sigma_{\zeta_{el-ref}-PI_{el}}} \quad (4)$$

Where the standard deviation of the difference between the reference scenario efficiency and the micro-cogeneration electrical performance index ($\sigma_{\zeta_{el-ref}-PI_{el}}$) can be found from equation 5.

$$\sigma_{\zeta_{el-ref}-PI_{el}} = \sqrt{\sigma^2_{PI_{el}} + \sigma^2_{\zeta_{el-ref}}} \quad (5)$$

Where if the uncertainty margins on each of ζ_{el-ref} and PI_{el} are known at a 95% confidence level ($U_{95,PI_{el}}$ and $U_{95,\zeta_{el-ref}}$), the standard deviations may be found from the following two equations.

$$\sigma_{PI_{el}} = \frac{U_{95,PI_{el}}}{1.96} \quad (6)$$

$$\sigma_{\zeta_{el-ref}} = \frac{U_{95,\zeta_{el-ref}}}{1.96} \quad (7)$$

To perform such an analysis, all of the uncertainties propagated from the models used to represent the various components in the micro-cogeneration case must be accounted for along with those of the reference scenario. Such a detailed accounting will be provided in the following sections. Throughout this analysis, in some cases, assumptions were used when it was not possible to evaluate either a parameter value or its uncertainty. The sensitivity of the results to these assumptions is described in Section 4.1. To begin, in the next section, a more detailed description of the plant networks to be considered as a case study to demonstrate the methodology developed in this article is provided.

3. Plant Network

As a case study, this article will focus on the comparison of the energy performance between the two plant networks shown in Figure 1: a plant network representing the micro-cogeneration case and another representing the reference scenario. It is important to understand that both considered the same DHW profile on an energy basis. For every simulation time-step, the same amount of energy consumption was drawn from the TWH in the reference scenario as was drawn from the tank/auxiliary heater in the micro-cogeneration case.

The DHW profiles that were used in simulations were obtained from Edwards et al. [51]. These profiles are at a 5-minute timescale resolution and a 1 L DHW draw resolution. 12 DHW profiles were obtained, each containing 1 year's worth of data, A summary of the DHW consumption for each of these 12 DHW profiles is shown in Table 1 in both a volumetric (L day^{-1}) and energy (MJ day^{-1}) basis. Note that the house identifiers (H5, H11, H14 etc.) shown in Table 1 are not sequential but do correspond to the naming convention of the 12 profiles Edwards et al. [51] made available. To convert the profiles from a volumetric to an energy basis, a constant outlet temperature of 55 ^{o}C was assumed along with an assumed monthly mains temperature profile shown at the bottom of Table 1. All simulations were conducted for the entire year.

The PEMFC obtains its natural gas fuel supply from the local gas distribution network. In the PEMFC micro-cogeneration case, the AC bus can interface with the electrical grid. Net AC output from the PEMFC can be consumed locally by the occupants or exported to the grid if there is excess production. The occupants can also consume grid electricity when the PEMFC's output is less than the occupants' demands. Note that if excess production can be exported, and for the

Table 1: Summary of simulated individual DHW draw profiles

House	H5	H11	H14	H16	H35	H38	H43	H49	H52	H59	H69	H73
DHW (L day^{-1})	166	118	189	124	246	176	116	169	240	219	170	182
DHW (MJ day^{-1})	30	22	34	23	45	32	21	31	44	40	31	33
Month	1	2	3	4	5	6	7	8	9	10	11	12
mains (^{o}C)	6.55	5.77	6.55	8.69	11.61	14.53	16.67	17.46	16.67	14.53	11.61	8.69
outlet (^{o}C)	55	55	55	55	55	55	55	55	55	55	55	55

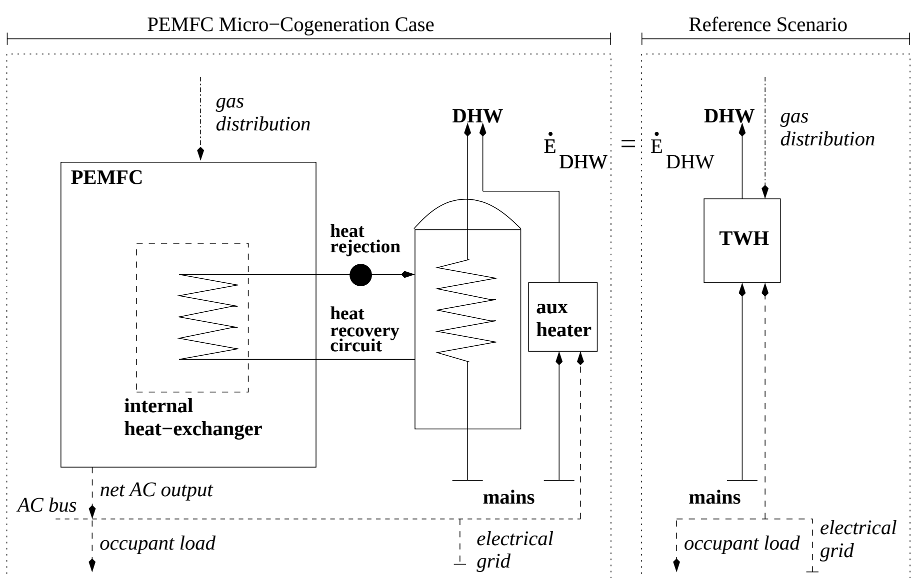

Figure 1: Micro-cogeneration plant network to be used in simulations

control mode that was simulated (described in Section 3.5), only the difference between the occupant demands for electricity between the reference scenario and the micro-cogeneration case needs to be considered. This difference is only caused by the difference between the electricity consumption of the TWH in the reference scenario and the auxiliary heater in the micro-cogeneration case. For this reason, other occupant electricity demands were not explicitly considered in the analysis but the difference in heater consumption was (in equation 8).

In the heat-recovery circuit, the thermal output obtained from the PEMFC's internal heat exchanger is circulated to a storage tank. When the incoming water's temperature to the internal-heat exchanger exceeds its limit of 59.1 ^oC, the PEMFC's thermal output is rejected.

DHW is drawn from the storage tank. For cases where the storage tank's temperature is less than 45 ^oC and is insufficient to meet occupants' thermal comfort demands, the DHW is drawn from an auxiliary heater. It was later found in the simulations in Section 4 that when DHW consumption was less than 50 MJ day^{-1} this auxiliary heater provided less than 1% of the DHW demand and electrical production. Since it was rarely used in the most important region of DHW usage, it was conservatively assumed to be an electrical resistive heater that was powered from the electrical grid and was not modelled in detail. The sensitivity of the results to this conservative assumption will be discussed in Section 4.1.

As was mentioned by Johnson et al. [3], a reasonable reference scenario that the PEMFC micro-cogeneration case should be compared to is where the occupants' load is entirely met by the electrical grid and an efficient reference gas-fired heater. It has been shown [52, 53] that the most efficient conventional method of providing DHW is with a gas-fired condensing TWH. This is the type of heater that was considered in these simulations.

For the particular micro-cogeneration case and reference scenario described in this section, PI_{el} from equation 1 can be expressed by equation 8.

$$PI_{el} = \frac{E_{fc-ac} + E_{el-TWH} - E_{el-aux}}{E_{fc-fuel} - E_{fuel-TWH}} \tag{8}$$

Where E_{fc-ac} is the AC electricity production in kJ. E_{el-aux} is the electricity consumption of the auxiliary heater in kJ. E_{el-TWH} is the electricity consumption of the TWH in kJ. $E_{fc-fuel}$ is the energy of the fuel consumption of the PEMFC in kJ. $E_{fuel-TWH}$ is the energy of the fuel consumption of the TWH in kJ.

3.1. PEMFC Model

Although the data presented by Johnson et al. [5] are the most reliable, the associated model was intended for general purpose use so it was calibrated over a broad range of operating conditions with detailed subcomponent models. However, for the specific purpose under consideration here, the exact operating range was known along with the specific model outputs required. For these reasons, several adaptations were made to the model presented by Johnson et al. [5]. These adaptations are described as follows.

First, a new model equation that directly describes the relationship between the PEMFC's net DC output (P_{fc-dc} in W) and AC output (P_{fc-ac} in W) was derived. This was to allow for a more direct calculation of PI_{el} in equation 8. This equation is shown below.

$$P_{fc-ac} = e_0 + e_1 \cdot P_{fc-dc} \tag{9}$$

Where e_i are the model calibration coefficients given in Table 2.

Second, a new model equation that directly describes the relationship between the PEMFC's net DC output (P_{fc-dc} in W) and fuel consumption ($\dot{E}_{fc-fuel}$ in W) was derived. Again, this was to allow for a more direct calculation of PI_{el} in equation 8. This equation is shown below.

$$\dot{E}_{fc-fuel} = f_0 + f_1 \cdot P_{fc-dc} + f_2 \cdot P_{fc-dc}^2 \tag{10}$$

Where f_i are the model calibration coefficients given in Table 2.

The final adaptation is that only data that were within the range of temperatures at the PEMFC inlet in the heat-recovery circuit (T_{fc-in} in ^{o}C) permissible in the simulations were used to calibrate this model. This was to ensure more accurate model fits to reduce model prediction uncertainties (described in Table 3). The model equation is shown below.

$$q_{fc} = r_0 + r_1 \cdot P_{fc-dc}^{\alpha_0} + r_2 \cdot (T_{fc-in} - T_0)^{\alpha_1} \tag{11}$$

Where r_i and α_i are the model calibration coefficients given in Table 2.

Table 3 describes the uncertainty margins that were displayed graphically by Johnson et al. [5] in the measurement uncertainty column. Beside it are the prediction uncertainties associated with using equations 9 to 11.

Here the prediction uncertainties are taken as the maximum residual observed between a measured value and a model prediction. For each parameter, all uncertainties shown in Table 3 were treated as independent sources of bias (b_{i,Φ_k}) and were combined into a total bias B_{Φ_k} for the kth parameter Φ_k according to the following equation given by Moffat [54].

$$B_{\Phi_k} = \sqrt{\sum_i (b_{i,\Phi_k}^2)} \tag{12}$$

Table 2: Calibration coefficients for the PEMFC model derived from the data obtained by Johnson et al. [5]

AC output parameters for Equation 9	$e_0 = -4.276677$; $e_1 = 8.910647 \cdot 10^{-1}$;
FCPM fuel consumption coefficients for Equation 10	$f_0 = 432.73315$; $f_1 = 1.21272$; $f_2 = 9.8793471 \cdot 10^{-4}$;
Heat recovery parameters for Equation 11	$r_0 = 2.340002 \cdot 10^2$; $r_1 = 1.7938934 \cdot 10^{-2}$; $r_2 = -1.7851876 \cdot 10^{-1}$; $\alpha_0 = 1.6$; $\alpha_1 = 2$; $T_0 = 26.5$;
Range of applicability: $40^oC \leq T_{fc-in} \leq 59.1^oC$ $315\ W \leq P_{fc-dc} \leq 1110\ W$ $T_{room} \approx 22^oC$	

Table 3: PEMFC model parameter and prediction uncertainties based on the data obtained by Johnson et al. [5]

Parameter Φ_k	**Measurement Uncertainty**	**Prediction Uncertainty**
	b_{i,Φ_k}	
P_{fc-dc}	$\pm 0.7\% P_{fc-dc}$	
P_{fc-ac}	$\pm 3.2\% P_{fc-ac}$, ± 13.4 W	± 10.4 W
$\dot{E}_{fc-fuel}$	$\pm 1.2\% \dot{E}_{fc-fuel}$	± 43.3 W
q_{fc}	± 41.2 W	± 54.1 W
T_{fc-in}	$\pm 0.8\ ^o$C	

The total bias of each individual parameter was then propagated to calculate an overall bias for on $B_{PI_{el}}$ according to the following equation.

$$B_{PI_{el}} = \sqrt{\sum \left(\frac{\partial PI_{el}}{\partial \Phi_k} \cdot B_{\Phi_k} \right)^2} \tag{13}$$

For the purposes here, $B_{PI_{el}}$ will be considered as the 95% confidence intervals ($U_{95,PI_{el}}$) of the simulation results for a particular DHW profile.

To demonstrate how the uncertainties in Table 3 were propagated to simulation results consider, for example, the uncertainties associated with P_{fc-ac}. For each simulation, P_{fc-ac} was determined at each time-step and an average value ($\bar{P}_{fc-ac}$) was determined for the entire annual simulation. For this case, equation 12 was evaluated using equation 14 with the individual uncertainties from Table 3.

$$B_{P_{fc-ac}} = \sqrt{\left(0.032 \cdot \bar{P}_{fc-ac}\right)^2 + (13.4 \text{ W})^2 + (10.4 \text{ W})^2} \tag{14}$$

Since PI_{el} from equation 8 is expressed in terms of energy, $B_{P_{fc-ac}}$ must be multiplied by the simulation's duration (Δt) as shown in Equation 15.

$$B_{E_{fc-ac}} = B_{P_{fc-ac}} \cdot \Delta t \tag{15}$$

To propagate $B_{E_{fc-ac}}$ to $B_{PI_{el}}$ using equation 13, the sensitivity of $B_{PI_{el}}$ with respect to E_{fc-ac} ($\frac{\partial PI_{el}}{\partial E_{fc-ac}}$) was calculated using equation 16.

$$\frac{\partial PI_{el}}{\partial E_{fc-ac}} = \frac{1}{E_{fc-fuel} - E_{fuel-TWH}} \tag{16}$$

Similar procedures were performed for all of the other uncertainties described in Table 3. Afterwards, they were all combined according to equation 13.

3.2. Storage Tank

The storage tank shown in Figure 1 was modelled using a lumped-heat-capacity approximation. This approximation neglects any effects of thermal stratification within the tank. This is a conservative assumption since, if stratification were considered, cooler water at the bottom of the tank could be used to supply the inlet of the PEMFC's internal heat exchanger to increase the amount of heat recovered. The sensitivity of the results to this conservative assumption will be discussed in Section 4.1.

The standing loss of the tank (q_{loss}) was calculated based on a cylindrical geometry, with a height-to-diameter ratio of 1.25 and a heat-loss coefficient of 0.38 Wm^{-2} $^oC^{-1}$ (corresponding to 10 cm of fiberglass insulation [7]) in an ambient environment of 18 ^oC.

3.3. Tankless Water Heater Model

For the reference scenario, the condensing TWH model developed by Johnson and Beausoleil-Morrison [55] was used to predict its gas energy consumption. The individual uncertainties in the calibration parameters propagated to an overall model uncertainty for predictions of $E_{TWH}\pm$ 5.5%. It is also apparent that this model consistently under-predicts the energy consumption compared to the data from heaters measured in practice that it was validated against. At a maximum, the under-prediction was 8.7% in the region of interest here. Conservatively, this amount will be ignored. The sensitivity of the results to this conservative assumption will be discussed in Section 4.1.

Also Johnson and Beausoleil-Morrison [55] predicted E_{TWH} based on DHW draw data gathered at a 1-second timescale resolution that were obtained from Bohac et al. [52]. For these simulations here, to estimate the effect that using DHW data of coarser resolution has, the profiles from Bohac et al. [52] were coarsened to a 5-minute timescale resolution and a 1 L draw resolution. When model predictions for E_{TWH} were compared at the two different resolutions, it was found that E_{TWH} at the coarser resolution should be multiplied by a factor of 1.016±0.015 for daily DHW energy consumption greater than 30 MJ day^{-1}.

The electricity consumption of the TWH (E_{el-TWH}) was also considered. This was modelled according to a relationship that was derived from data presented by Hoeschele and Weitzel [53] for a condensing TWH and is presented below in the following equation.

$$E_{el-TWH}(\text{MJ day}^{-1}) = 0.446 + 0.0147 \cdot E_{DHW}(\text{MJ day}^{-1}) \tag{17}$$

Equation 17 expresses the electricity consumption as the sum of a fixed consumption and an amount of consumption that is related to the amount of daily DHW energy consumption (E_{DHW}). To evaluate the difference between the amount of electricity consumption of the TWH in the reference scenario and the auxiliary heater in the micro-cogeneration case ($E_{el-TWH} - E_{el-aux}$) in equation 8, it is assumed that the fixed consumption is the same in both scenarios, therefore, only the term related to use ($0.0147 \cdot E_{DHW}$) was explicitly calculated. The overall contribution of this term is small to the numerator in equation 8. Therefore, its associated uncertainty was neglected.

It should also be noted that E_{TWH} predicted by this model is based on the higher heating value (HHV) of natural gas at 15 ^{o}C and 101.325 kPa. To convert from this heating value reference to be consistent with the one used by Johnson et al. [5] (LHV at 25 ^{o}C and 101.325 kPa) a factor of 1.11 is appropriate based on heating values calculated from standard enthalpies of formation and the Shomate equation [56] for the combustion reaction of methane.

3.4. Reference Electrical Efficiency

The electrical efficiency ($\zeta_{el-plant}$) of a central gas plant is given by equation 18.

$$\zeta_{el-plant} = \frac{E_{el-ref}}{E_{fuel-ref}} \tag{18}$$

Where the net electrical output (E_{el-ref}) and the energy content of the fuel consumed ($E_{fuel-ref}$) must be known.

Data from the Independent Electricity System Operator [57] can be used to estimate the net electrical output for any plant in Ontario. To estimate the fuel consumption for each plant, data from Environment Canada [58] can be used.

Environment Canada [58] does not publish fuel consumption directly, rather, they publish CO_2 emissions (both direct and total equivalent) for all major emitters, including central gas plants, who have a legal obligation to report their emissions. If it is assumed that all of the direct CO_2 emissions from a gas plant are caused by the consumption of gas for power generation, the energy content of the fuel consumed can be found by equation 19.

$$E_{fuel-ref} = \frac{m_{CO_2-ref}}{EF_{CO_2}} \tag{19}$$

Where EF is the emissions factor associated with a pollutant and is normally given as a ratio of the mass of pollutant (CO_2) produced for the energy content of the fuel consumed. The MOE [59] gives the value for the emissions factor for CO_2 for the consumption of natural gas for electricity generation according to equation 20.

$$EF_{CO_2} = 49.03 \text{ kg GJ}^{-1} \tag{20}$$

This analysis can also be performed with a facility's reported CH_4 and NO_2 emissions with corresponding emissions factors (EF_{CH_4} = 12.79 g GJ^{-1} and EF_{NO_2} =

1.279 g GJ^{-1}). For the plant eventually selected to represent the reference scenario (described later in Table 4), an identical value for E_{fuel} is obtained if the analysis is performed using their reported CO_2, CH_4 or NO_2 emissions with the corresponding emissions factor from 2011-2013. Therefore, it is reasonable to conclude that these are the exact emissions factors this plant used to estimate their emissions from their known fuel consumption. It is important to understand that by knowing these values exactly, this plant's conversion of their known fuel consumption to emissions can be undone. Therefore, uncertainty associated with these emissions factors can be omitted from the uncertainty analysis performed later.

For the uncertainty analysis performed later, it is important to determine with what uncertainty a plant might know their value of $E_{fuel-ref}$ to be. They determine this value according to equation 21.

$$E_{fuel-ref} = V_{fuel-ref} \cdot HHV \tag{21}$$

A plant determines $E_{fuel-ref}$ as the product of both the volume of fuel ($V_{fuel-ref}$) it consumes and its higher heating value (HHV) at a standard reference condition of 101.325 kPa and $15^{o}C$. The Canadian Department of Justice [60] requires that the volume of gas sold by utilities to be accurate to within 3%. This value will be considered as the uncertainty of $V_{fuel-ref}$.

Greater uncertainty is associated with the HHV. The MOE [59] allows for natural gas fired plants to obtain their heating value using one of two methods. In the first method, they obtain a value from their supply utility. The two major gas supply utilities in Ontario each reported a 6-month average HHV twice a year, each year from 2011 - 2013 for emissions reporting purposes. In this period, every reported value from each utility was 38 MJ m^{-3}. The MOE provided these values when contacted. However, these values are not site specific and some variation in the HHV between sites is expected.

In the second method, they obtain a value from on-site measurements at the plant. If the HHV is measured on-site at a plant, the MOE [59] allows for the HHV to be determined as inaccurate as $\pm$ 5%. As the emissions reporting guideline [59] is written, this uncertainty only applies to this second method, however, it is still an indication of what uncertainty the MOE [59] considers to be acceptable. Also, the MOE [59] specifies that the HHV of natural gas should be between 36.3 and 40.98 MJ m^{-3}. If an HHV of 38 MJ m^{-3} $\pm$5% is assumed, the lower uncertainty margin (36.1 MJ m^{-3}) nearly coincides with the lower limit of what is permissible. However, the agreement between the upper uncertainty margin (39.9 MJ m^{-3}) and the upper limit of what is permissible is not as close. Notwithstanding this limitation, these considerations indicate that an uncertainty of $\pm$ 5% is reasonable for the HHV and this value will be assumed.

Table 4 describes the calculation of the highest electrical efficiency observed from a combined-cycle plant in Ontario, from 2011 to 2013. The bias of $\pm$ 5% for the HHV [59] combined with the bias of $\pm$ 3% for $V_{fuel-ref}$ [60] account for the uncertainty of the energy content associated with fuel consumption as described earlier. The IESO [57] reported the uncertainty of their generator output data as $\pm$ 10 MW. It is assumed that the IESO [57] knows when a plant is operating with negligible uncertainty. The yearly variation is a measure of the maximum amount that the efficiency in any single year may deviate from the value at the bottom of Table 4 (the 3-year efficiency) for a single plant. As there were only 3 years of available data for each plant, the sample was extended to the 6 largest combined-cycle plants without cogeneration in Ontario to determine the value shown for the yearly variation. The uncertainties of the energy content of fuel consumption, the yearly variation and the electrical production are combined to yield the uncertainty of the electrical efficiency shown at the bottom of Table 4.

Table 4: Calculated reference electrical efficiency for a high-efficiency combined-cycle plant in Ontario, Canada from 2011 to 2013 and uncertainty margins

Parameter Description	**Value**	**Uncertainty**
Average Output	314.58 MW	± 10 MW
Hours of Operation	10013 hrs	none
Energy Content of Fuel Consumption (LHV)	21.30 PJ	±5%,3%
Yearly Variation		± 4%
Electrical Efficiency	0.5323	± 0.041

In comparison to a central gas plant, one advantage of a micro-cogeneration system that should be considered is that its electrical production is close in proximity to where it will be consumed. Therefore, a micro-cogeneration system will make no use of the electrical transmission system and limited use of the distribution system.

As data were publicly available from the IESO [61] that described the hourly losses in the electrical transmission system in Ontario, the efficiency of the transmission system was calculated. This was done considering an entire year's worth of data, sampled every hour, for 2008 and 2013. The resulting transmission efficiency was 97.4%. The associated precision index [54] was negligible.

Unfortunately, similar data relevant to the distribution system in Ontario were not available. Distribution efficiency estimates based on a modelling approach

[62] for an urban consumer have shown this value to be approximately 96.7%.

The following equation defines the reference electrical efficiency that was considered against which the micro-cogeneration system was compared to.

$$\zeta_{el-ref} = \zeta_{el-plant} \cdot \zeta_{el-t} \cdot \zeta_{el-d} = 0.5014 \pm 0.039 \quad (22)$$

In equation 22, the reference electrical efficiency (ζ_{el-ref}) was defined as the product of the central combined-cycle plant efficiency ($\zeta_{el-plant}$), the electrical transmission system efficiency (ζ_{el-t}) and the distribution system efficiency (ζ_{el-d}). The value at the far right of equation 22 was the 95% confidence interval ($U_{95,\zeta_{el-ref}}$) used to determine the standard deviation in equation 7.

It is important to consider that a micro-cogeneration system may make some use of the distribution system if not all of its electrical production can be consumed in close proximity to where it is located. It is also important to consider that a substantial portion of the losses within the distribution system in urban Ontario are no-load losses that are not directly related to its load and only to the system's existence. To investigate the effect of this, the sensitivity of the results when fewer losses in the distribution system are considered (ζ_{el-d} is increased) is discussed in Section 4.1.

3.5. Control Mode

The particular control mode that was selected represents an attempt to maximize the potential benefit of a micro-cogeneration system by minimizing the amount of gas energy consumed to meet the total energy demand of a residential occupant for the case where micro-cogeneration is used relative to the reference scenario ($\Delta\dot{E}_{gas}$) as shown in equation 23.

$$\Delta\dot{E}_{gas} = \dot{E}_{fc-fuel} - \frac{1}{\zeta_{el-ref}} \cdot P_{fc-ac} - \frac{q_{fc}}{\zeta_{TWH}} \cdot \Psi \tag{23}$$

Because not all of the thermal output of a PEMFC can be used for DHW (a portion is rejected), q_{fc} is multiplied by a factor (Ψ) in equation 23 that represents the percentage of q_{fc} that may eventually be used for DHW.

At each simulation time-step, the value of P_{fc-dc} that was selected was that which minimized equation 23. For this, ζ_{TWH} was taken as a constant 100%. The electric consumption of the auxiliary heater was also ignored.

In these simulations, the expression for Ψ to be used in equation 23 was only approximated. The expression for Ψ that was chosen is given by equation 24.

$$\Psi(T_{Tank}) = \begin{cases} 0, & T_{Tank} \geq 59.1^oC \\ \Psi_0 \cdot (59.1^oC - T_{Tank}), & 59.1^oC > T_{Tank} > T^* \\ 1, & T^* > T_{Tank} \end{cases} \tag{24}$$

The preceding equation assumed that if the tank temperature increased above the maximum permissible value of the PEMFC heat recovery circuit then none of the heat recovered was useful. Below a certain temperature (T^*), all of the heat recovered was useful. Between these two temperatures there was a linear transition region where Ψ_0 was a parameter determined from optimization. For the preceding equation $T^* = 59.1^oC - \Psi_0^{-1}$.

For the optimization procedure, a Hooke-Jeeves algorithm [63] was used. As the most profligate of the 12 profiles only demanded approximately 45 MJ day^{-1} of DHW in the simulated year, to estimate how demands of greater consumption levels might have performed, every combination of 2 of the 12 profiles was also considered in these simulations. In total, 78 DHW profiles were simulated. The profiles that are combinations are representative of the DHW demand that would be appropriate for a load sharing application between two sets of occupants.

The objective of the optimization was to maximize the average PI_{el} of three of the 78 DHW profiles. The three selected profiles had DHW consumptions of approximately 50 MJ day^{-1}. This optimization process was also repeated for a group of consumers with 40 MJ day^{-1} of DHW consumption. Although the optimized parameters determined from this were slightly different, the results described in Section 4 were insensitive to these alternative values so they were not used.

The optimum storage tank volume found from the 50 MJ day^{-1} consumption profiles was 1500 L and Ψ_0 was determined to be 0.06 $^oC^{-1}$. These optimized parameters were effective at reducing the amount of heat rejected to zero for all simulated DHW profiles with greater than 35 MJ day^{-1} of consumption, however, the standing loss of the tank was approximately 8 MJ day^{-1} for all cases.

4. Results

The results from 1 sample day for 1 of the 78 domestic hot water profiles that was simulated are shown in Figure 2. For this sample profile, the daily average DHW consumption was approximately 40 MJ day^{-1}. At the top of this figure, the temperature of the storage tank and TWH are plotted. At the bottom of this figure, the rates of various energy inputs and outputs relevant to the plant network shown in Figure 1 are plotted. The top and bottom of this figure share a common abscissa that represents the number of minutes from the start of this sample day.

For the graph at the bottom of Figure 2, note that the ordinate on the left side of this graph applies to the rates of energy input and output for the TWH. Also note that the rate of energy output for the TWH is equivalent to that of the DHW drawn in a particular time step. Here a single DHW draw is defined as a continuous period of time over which DHW is drawn. Only the average rate of energy input and output over a DHW draw are plotted.

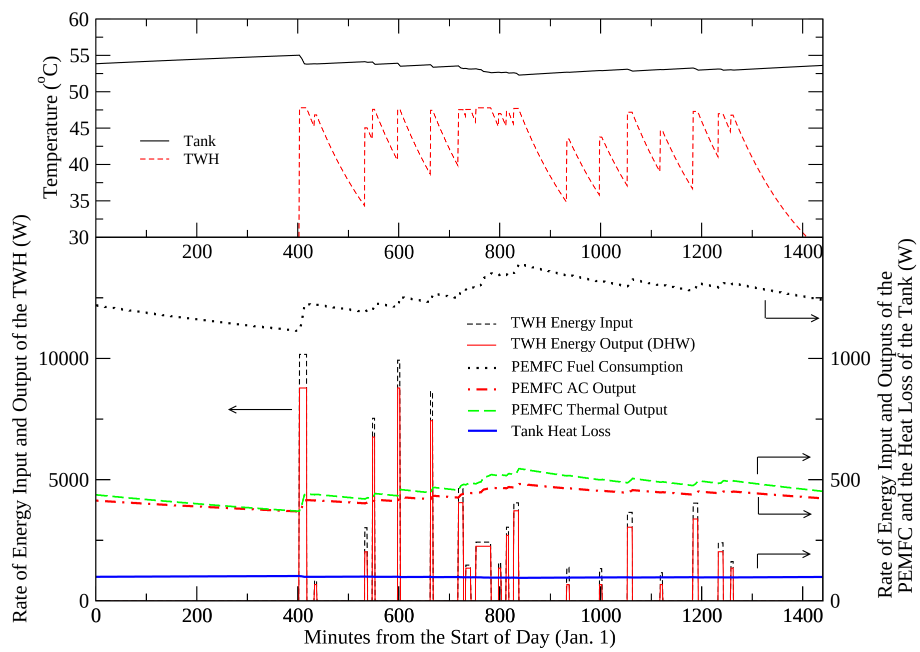

Figure 2: Temporal results for 1 sample day for 1 of the 78 domestic hot water profiles that was simulated

The ordinate on the right side the graph at the bottom of Figure 2 applies to all the other series plotted on this graph (PEMFC fuel consumption, PEMFC AC output, PEMFC thermal output and heat loss of the tank). This second ordinate was only necessary so that these other series could be represented on the same graph as the TWH input and output that are an order of magnitude greater.

For periods of time between DHW draws, it can be seen that the tank's temperature rises slowly while the TWH's temperature decays exponentially. The result from this slow increase in tank temperature is that the control mode directs the PEMFC to modulate its output so that its fuel consumption, thermal and AC output decrease at a similar rate. While difficult to resolve from the scale of the graph, the tank's temperature increase during these periods also causes the heat loss to increase as well.

During DHW draw periods, the temperature of the tank decreases suddenly. The result from this is that the control mode directs the PEMFC to modulate its output so that its fuel consumption, thermal and AC output increase suddenly as well. The TWH temperature suddenly rises during these periods to reach its setpoint. During these firing periods, the TWH temperature at the end of each firing period is shown to represent the temperature of the TWH for the entire firing period.

The results of the simulations of the 78 DHW profiles with the optimized model parameters are shown in Figure 3. The DHW consumption of each profile is shown along the abscissa while the PI_{el} of the micro-cogeneration system and its corresponding $p(\zeta_{el-ref} > PI_{el})$ are shown along the ordinates. The error bars shown on the PI_{el} markers represent the 95% uncertainty margins.

As can be seen from Figure 3, the PI_{el} of the micro-cogeneration case begins to exceed ζ_{ref-el} for DHW consumption levels greater than approximately 35 MJ day^{-1}. However, when uncertainty margins are taken into account, the PI_{el} reliably ($p(\zeta_{el-ref} > PI_{el}) < 0.05$) outperforms the reference scenario when DHW consumption exceeds 50 MJ day^{-1}. Only a load sharing profile is the type of profile at this threshold.

The major reason that PI_{el} increases from DHW consumption levels of ap-

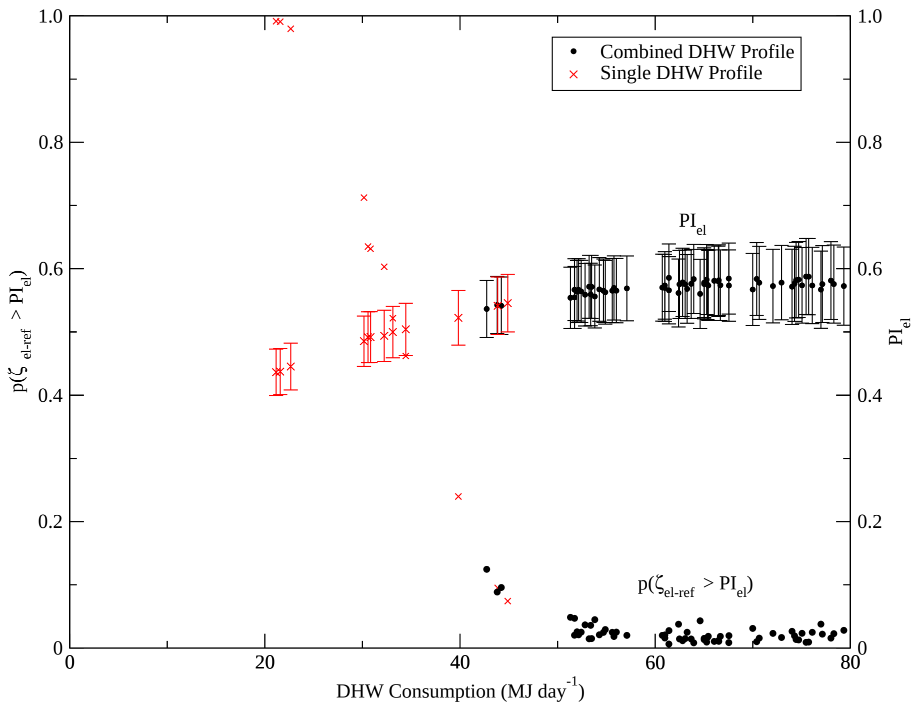

Figure 3: PEMFC electrical performance index and the probability that it does not exceed the reference electrical efficiency versus DHW consumption

proximately 20 to 60 MJ day^{-1} is because of the tank's temperature. At lower consumption levels, the tank's temperature is elevated. The negative value of the r_2 coefficient in Table 2 indicates a decrease in thermal output (q_{fc}) at elevated temperatures. Also at elevated tank temperatures, the control mode described by equation 23 reduces the PEMFC's electrical output set-point (P_{fc-dc}) to avoid wasting its thermal output. However, at reduced electrical output set-points the PEMFC's thermal and electrical efficiencies are also reduced. Also at reduced electrical output set-points, the tank's loss of 8 MJ day^{-1} constitutes a more substantial portion of the thermal output of the PEMFC, therefore, a lower proportion of the PEMFC's thermal output is being used to serve DHW. Above 60 MJ day^{-1} PI_{el} does not increase substantially. However, this is mainly due to the fact that this particular series of simulations has been optimized for 50 MJ day^{-1} of consumption.

4.1. Sensitivity of Results to Assumptions

To investigate how other assumptions might influence the aforementioned results, the following analyses were performed for several sensitivity cases. For each of the following sensitivity cases, first a different assumption was made. This was followed by an optimization to determine Ψ_0 and V_{tank} under the different assumption. The simulations were then performed with the different assumption to determine the DHW consumption level where $p(\zeta_{el-ref} > PI_{el}) < 0.05$. Figure 4 displays the p-Value of each of the examined sensitivity cases for each of the 78 DHW profiles that were simulated against DHW consumption. Each separate case is shown as a separate series and is denoted with a case number. These cases are described in the following paragraphs. Note that the base case in Figure 4 refers to the simulations whose results were described in the preceding section.

Also shown on Figure 4 is a horizontal dotted line at $p(\zeta_{el-ref} > PI_{el}) = 0.05$.

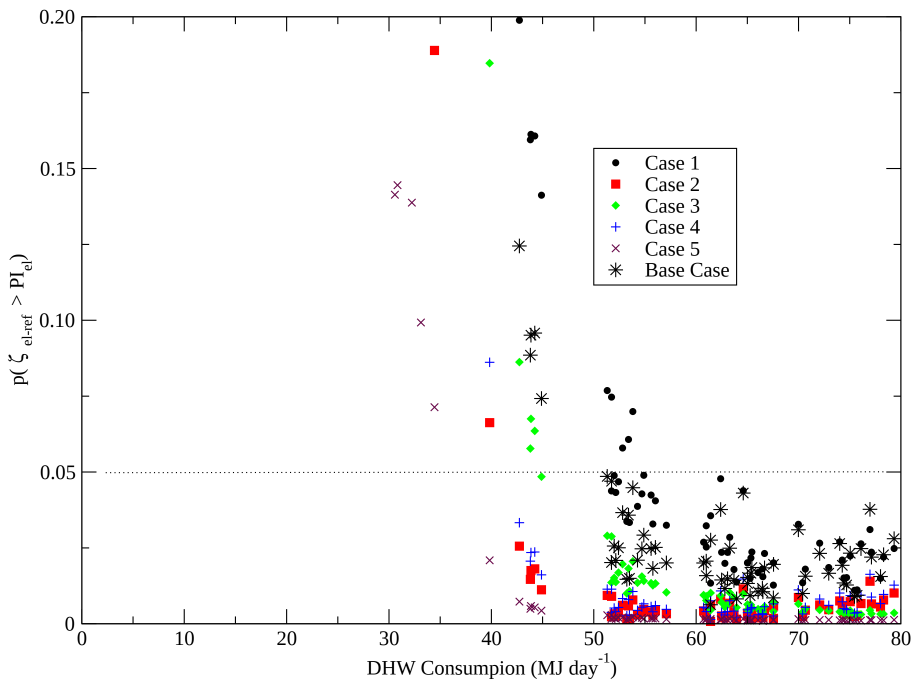

Figure 4: The probability that the electrical performance index does not exceed the reference electrical efficiency versus DHW consumption for each of the sensitivity cases that were considered along with the base case.

Some distribution loss may not be avoided by using a micro-cogeneration system. As a more conservative assumption, only half of the benefit the distribution efficiency provides was considered (Case 1). Under this assumption, it was found that at 55 MJ day^{-1} of DHW consumption the micro-cogeneration case reliably outperforms the reference scenario ($p(\zeta_{el-ref} > PI_{el}) < 0.05$).

The TWH model may be over-predicting its energy input by as much as 8.7% in the DHW consumption regions of interest here. As a less conservative assumption, E_{TWH} was multiplied by 1/(1-0.087) (Case 2). Under this assumption, it was found that at 42 MJ day^{-1} of DHW consumption the micro-cogeneration case reliably outperforms the reference scenario ($p(\zeta_{el-ref} > PI_{el}) < 0.05$).

The auxiliary heater was assumed to be an electrical resistance heater. As a less-conservative assumption, it was assumed to be a natural gas heater with 100% efficiency (HHV) (Case 3). Under this assumption, it was found that at 45 MJ day^{-1} of DHW consumption the micro-cogeneration case reliably outperforms the reference scenario ($p(\zeta_{el-ref} > PI_{el}) < 0.05$).

Tank stratification might influence this analysis. As a less-conservative assumption, the water inlet temperature of the fuel cell was always set to 40 ^{o}C (Case 4). Below this value the amount of thermal output recovered does not increase substantially. Under this assumption, it was found that at 42 MJ day^{-1} of DHW consumption the micro-cogeneration case reliably outperforms the reference scenario ($p(\zeta_{el-ref} > PI_{el}) < 0.05$). Tank stratification might also allow the tank's size to be reduced since colder water at the bottom of the tank could be used to supply the PEMFC and would, therefore, allow the average tank temperature where heat rejection occurs to be increased above 59.1^{o}C. This increases the amount of energy that can be stored within a tank of a given size. Modelling this aspect would require a more sophisticated tank model than the lumped-heat-capacity approximation used. However, the objective of this research was to develop a methodology to evaluate the energy potential of a fuel-cell system that considers model uncertainties and to demonstrate its utility. Since the results from the preceding section clearly demonstrated that by ignoring uncertainties dubious conclusions can be drawn (i.e. that the considered micro-cogeneration case is more efficient than the reference at average levels of DHW consumption), performing simulations with a stratified tank model was considered outside of the scope of this present research.

When all 3 previous less conservative assumptions were applied to the same simulation (Case 5), after optimization, it was found that at 38 MJ day^{-1} of DHW consumption the micro-cogeneration case reliably outperforms the reference scenario ($p(\zeta_{el-ref} > PI_{el}) < 0.05$). While this is characteristic of an average DHW consumer, it represents an extremely optimistic scenario from the perspective of the micro-cogeneration system.

5. Conclusions

By considering the probability that the reference scenario outperformed the equivalent electrical performance index of the PEMFC micro-cogeneration case, a new methodology was developed to evaluate the energy performance of this type of system. The results of these simulations based on this methodology have established a range of DHW consumption values where the efficiency of the reference scenario has a low probability of exceeding the micro-cogeneration system's.

Had uncertainties been neglected, it would have been possible to conclude that the considered micro-cogeneration system was viable for serving only an average level of DHW consumption. However, when uncertainties were considered the analysis demonstrated that it is unlikely that the micro-cogeneration device considered here is viable in Ontario, Canada if its thermal output serves only domestic hot water needs; additional uses are required for the thermal output to make it viable (e.g. space heating or load sharing between houses). Therefore, uncertainties are an important aspect to consider in these types of analyses as they can significantly alter the conclusions that are drawn from them.

The methodology documented in this article can be repeated for other jurisdictions with models of other micro-cogeneration devices as they become available. Indeed, it would be interesting to analyze a device with a higher efficiency and/or a smaller capacity to determine whether micro-cogeneration servicing only domestic hot water needs can be viable for Ontario, Canada.

6. Acknowledgment

The authors would like to acknowledge the contributions of several members of Natural Resources Canada's CanmetENERGY lab's Buildings and Renewables Group: Gordon Mackenzie, Randy Biggs, Bruce Strathearn, Erik Thorsteinson and Tom Mackintosh in the design and commissioning of the experimental apparatus used to develop the fuel cell model used in this work and that of Mark Douglas for originally extending the invitation to participate in this collaborative effort and for providing helpful comments on this manuscript.

7. References

[1] Dorer, V., Weber, A.. Methodologies for the Performance Assessment of Residential Cogeneration Systems. IEA/ECBCS Annex 42 Report; 2007. ISBN No. 978-0-662-46951-3.

[2] EUROPA, . Commission implementing decision of December 19 2011 - establishing harmonised efficiency reference values for separate production of electricity and heat in application Directive 2004/8/EC of the European Parliament and of the Council and repealing Commission Decision 2007/74/EC. Official Journal of the European Union 2011;343:91–96.

[3] Johnson, G., Wills, A., Beausoleil-Morrison, I.. The proposal of a reasonable reference scenario for comparison with micro-cogeneration systems.

In: Proc. Fourth International Conference on Microgeneration and Related Technologies. Tokyo, Japan; 2015,.

[4] Staffell, I.. Zero carbon infinite COP heat from fuel cell CHP. Applied Energy 2015;147:373–385.

[5] Johnson, G., Beausoleil-Morrison, I., Strathearn, B., Thorsteinson, E., Mackintosh, T.. The calibration and validation of a model for simulating the thermal and electrical performance of a 1 kW_{AC} proton-exchange membrane fuel-cell micro-cogeneration device. Journal of Power Sources 2013;221(1):435–446.

[6] Beausoleil-Morrison, I., Lombardi, K.. The calibration of a model for simulating the thermal and electrical performance of a 2.8 kW_{AC} solid-oxide fuel-cell micro-cogeneration device. Journal of Power Sources 2009;186(1):67–79.

[7] Kopf, J.. The performance of residential micro-cogeneration coupled with thermal and electrical storage. Master's thesis; Carleton University; Ottawa Canada; 2012.

[8] McMurtry, S.. On configuration and control of the thermal plant for fuel-cell micro-cogeneration. Master's thesis; Carleton University; Ottawa Canada; 2013.

[9] Johnson, G., Kopf, J., Beausoleil-Morrison, I., Darcovich, K., Kenney, B., Mackintosh, T.. The annual performance of a fuel-cell based micro-cogeneration system with lithium-ion storage. In: Proc. Third International

Conference on Microgeneration and Related Technologies. Naples, Italy; 2013,.

[10] Han, Y., Beausoleil-Morrison, I., Wang, X.. Increasing the installation capacity of PV with PEMFC backup with a residential community. Energy Procedia 2015;78:675–680.

[11] Cao, S., Mohamed, A., Hasan, A., Sirén, K.. Energy matching analysis of on-site micro-cogeneration for a single-family house with thermal and electrical tracking strategies. Energy and Buildings 2014;68:351–363.

[12] Bianchi, M., De Pascale, A., Melino, F.. Performance analysis of an integrated CHP system with thermal and electric energy storage for residential application. Applied Energy 2013;112:928–938.

[13] Bianchi, M., De Pascale, A., Melino, F., Peretto, A.. Performance prediction of micro-CHP systems using simple virtual operating cycles. Applied Thermal Engineering 2014;71:771–770.

[14] Napoli, R., Gandiglio, M., Lanzini, A., Santarelli, M.. Techno-economic analysis of PEMFC and SOFC micro-CHP fuel systems for the residential sector. Energy and Buildings 2015;103:131–146.

[15] Yaji, S., Diarra, D.. Operating strategy of a solid oxide fuel cell system for a household energy demand profile. In: Proc. Third International Conference on Microgeneration and Related Technologies. Naples, Italy; 2013,.

[16] Vialetto, G., Noro, M., Rokni, M.. Innovative household systems based on solid oxide fuel cells for the Mediterranean climate. International Journal of Hydrogen Energy 2015;40:14378–14391.

[17] Rouholamini, M., Mohammadian, M.. Energy management of a grid-tied residential-scale hybrid renewable generation system incorporating fuel cell and electrolyzer. Energy and Buildings 2015;102:406–416.

[18] Zafar, S., Dincer, I.. Energy, exergy and exergoeconomic analyses of a combined renewable energy system for residential applications. Energy and Buildings 2014;71:68–79.

[19] Wakui, T., Wada, N., Yokoyama, R.. Energy-saving effect of a residential polymer electrolyte fuel cell cogeneration system combined with a plug-in hybrid electric vehicle. Energy Conversion and Management 2014;77:40–51.

[20] Windeknecht, M., Tzscheutschler, P.. Increasing electricity self-consumption of micro CHP-systems with electrically driven heater. In: Proc. Fourth International Conference on Microgeneration and Related Technologies. Tokyo, Japan; 2015,.

[21] Nakai, T., Okawa, I., Kosumi, T., Dobashi, R., Kurokawa, T., Uetsuji, A.. T-Grid System: electric power interchange system utilizing ene-farm in apartment. In: Proc. Fourth International Conference on Microgeneration and Related Technologies. Tokyo, Japan; 2015,.

[22] Sumiyoshi, D., Yamamoto, T., Hirata, T., Shigematsu, Y.. Installation effect estimation of fuel cells in an apartment by simulation analysis. In: Proc. Fourth International Conference on Microgeneration and Related Technologies. Tokyo, Japan; 2015,.

[23] Sommer, K.. Practical experience with a fuel cell unit for combined heat and power CHP generation at the building level. In: Proc. Fourth International Conference on Microgeneration and Related Technologies. Tokyo, Japan; 2015,.

[24] Gandiglio, M., Lanzini, A., Santarelli, M., Leone, P., Borchiellini, R.. Study of a low-temperature micro-cogeneration system with a proton exchange membrane fuel-cell for residential use. In: Proc. Third International Conference on Microgeneration and Related Technologies. Naples, Italy; 2013,.

[25] Gandiglio, M., Lanzini, A., Santarelli, M., Leone, P.. Design and optimization of a proton exchange membrane fuel cell CHP system for residential use. Energy and Buildings 2014;69:381–393.

[26] Cooper, S., Hammond, G., McManus, M., Ramallo-Gonzles, A., Rogers, J.. Effect of operating conditions on performance of domestic heating systems with heat pumps and fuel cell micro-cogeneration. Energy and Buildings 2014;70:52–60.

[27] Özgirgin, E., Devrim, Y., Albostan, A.. Modeling and simulation of a hybrid photovoltaic (PV) module-electrolyzer-PEM fuel cell system for micro-cogeneration applications. International Journal of Hydrogen Energy 2015;40:15336–15342.

[28] Fubara, T., Cecelja, F., Yang, A.. Modelling and selection of micro-CHP systems for domestic energy supply: The dimension of network-wide primary energy consumption. Applied Energy 2014;114:327–334.

[29] Nižetić, S., Tolj, I., Papadopoulos, A.. Hybrid energy fuel cell based system for household applications in a Mediterranean climate. Energy Conversion and Management 2015;105:1037–1045.

[30] Comodi, G., Cioccolanti, L., Renzi, M.. Modelling the Italian household sector at the municipal scale: Micro-CHP, renewables and energy efficiency. Energy 2014;68:92–103.

[31] Elmer, T., Worall, M., Wu, S., Riffat, S.. Emission and economic performance assessment of a solid oxide fuel cell micro-combined heat and power system in a domestic building. Applied Thermal Engineering 2015;90:1082–1089.

[32] Frazzica, A., Briguglio, N., Sapienza, A., Freni, A., Brunaccini, G., Antonucci, V., et al. Analysis of different heat pumping technologies integrating small scale solid oxide fuel cell system for more efficient building heating systems. International Journal of Hydrogen Energy 2015;40:14746–14756.

[33] Arsalis, A., Kær, S., Nielsen, M.. Modeling and optimization of a heat-pump-assisted high temperature proton exchange membrane fuel cell micro-combined-heat-and-power system for residential applications. Applied Energy 2015;147:569–581.

[34] Pellegrino, S., Lanzini, A., Leone, P.. Techno-economic and policy requirements for the market-entry of the fuel cell micro-CHP system in the residential sector. Applied Energy 2015;143:370–382.

[35] Yang, W., Zhao, Y., Liso, V., Brandon, N.. Optimal design and operation of a syngas-fuelled SOFC micro-CHP system for residential applications in different climate zones in China. Energy and Buildings 2014;80:613–622.

[36] Canelli, M., Entchev, E., Sasso, M., Yang, L., Ghorab, M.. Dynamic simulations of hybrid energy systems in load sharing application. Applied Thermal Engineering 2015;78:315–325.

[37] Thorsteinson, E., Strathearn, B., Mackenzie, G., Amow, G.. Permformance testing of a 1 kWe fuel cell cogeneration system. In: Proc. Second International Conference on Microgeneration and Related Technologies. Glasgow, Scotland; 2011,.

[38] Anindito, S., Entchev, E., Kang, E., Lee, E.. Implementation of spreadsheet modeling to compare the annual energy performance and cost of microgeneration systems. In: Proc. Third International Conference on Microgeneration and Related Technologies. Naples, Italy; 2013,.

[39] Entchev, E., Yang, L., Ghorab, M., Lee, E.. Simulation of hybrid renewable microgeneration systems in load sharing applications. Energy 2013;50:252–261.

[40] Ham, S., Jo, S., Dong, H., Jeong, J.. A simplified PEM fuel cell model for building cogeneration. Energy and Buildings 2015;107:213–225.

[41] Payne, R., Love, J., Kah, M.. CFCL's BlueGen product. Electrochemical Society Transactions 2011;35(1):81–85.

[42] Sommer, K., Mesenhöller, E.. Practical experience with a fuel cell unit

for combined heat and power (CHP) generation on the building level. The REHVA European HVAC Journal 2013;:12–16.

[43] Hody, S., Kanawaka, K., Thai, L.. Abilities of CFCL SOFC system in power modulation and charging of electric vehicle. In: Presentation. Fuel Cell Seminar and Energy Exposition. Orlando, USA; 2011,.

[44] Hody, S., Contreau, R., Dupe, C., Dupuis, D.. Feed back from Engie Lab (Crigen) and GRDF on some fuel cell micro-cogeneration systems installed on the field in France within the European program ENE.FIELD. In: Proc. Fourth International Conference on Microgeneration and Related Technologies. Tokyo, Japan; 2015,.

[45] Iwami, J., Higaki, K., Yasuhara, K., Suzuki, M., Uenoyama, S.. Development of a residential SOFC CHP system. In: Proc. Fourth International Conference on Microgeneration and Related Technologies. Tokyo, Japan; 2015,.

[46] Postlethwaite, O., Rogers, S., Selby, M.. Design for life - fuel cell power systems. In: Proc. Fourth International Conference on Microgeneration and Related Technologies. Tokyo, Japan; 2015,.

[47] Koda, J., Tairako, T., Sano, A., Yamada, K., Watanabe, T., Kobayashi, K.. Development of new model residential fuel cell systems. In: Proc. Fourth International Conference on Microgeneration and Related Technologies. Tokyo, Japan; 2015,.

[48] Watanabe, S., Tanaka, M., Koyama, Y., Hirai, K.. Development of resi-

dential 700W PEFC micro-CHP system. In: Proc. Fourth International Conference on Microgeneration and Related Technologies. Tokyo, Japan; 2015,.

[49] Tanaka, Y.. Development and demonstration of PV/FC/battery hybrid power system in Toyota City Low Carbon Society Project. In: Proc. Fourth International Conference on Microgeneration and Related Technologies. Tokyo, Japan; 2015,.

[50] Sasakura, H.. Next-generation household energy system demonstration at Next21 experimental multi-unit housing complex. In: Proc. Fourth International Conference on Microgeneration and Related Technologies. Tokyo, Japan; 2015,.

[51] Edwards, S., Beausoleil-Morrison, I., Laperrière, A.. Representative hot water draw profiles at high temporal resolution for simulating the performance of solar thermal systems. Solar Energy 2015;111:43–52.

[52] Bohac, D., Schoenbauer, B., Hewett, M., Lobenstein, M., Butcher, T.. Actual savings and performance of natural gas tankless water heaters. Tech. Rep.; Center for Energy and Environment; 2010.

[53] Hoeschele, M., Weitzel, E.. Monitored performance of advanced gas water heaters in California homes. ASHRAE Transactions 2013;119:214–225.

[54] Moffat, R.. Describing the uncertainties in experimental results. Experimental Thermal and Fluid Science 1988;1:3–17.

[55] Johnson, G., Beausoleil-Morrison, I.. The calibration and validation of a model for predicting the performance of gas-fired tankless water heaters in domestic hot water applications. Applied Energy 2016;177:740–750.

[56] NIST, . Nist chemistry webbook. Tech. Rep.; National Institute of Standards and Technology; 2016. http://webbook.nist.gov/ - Accessed Aug. 2016.

[57] IESO, . Generators output and capability report. Tech. Rep.; Independent Electricity System Operator; 2013. http://reports.ieso.ca/public/GenOutputCapability/ - Accessed Aug. 2016.

[58] Environment Canada, . Greenhouse gas emission reporting program online data search - facility reported data. Tech. Rep.; Environment Canada; 2014. http://www.ec.gc.ca/ges-ghg/donnees-data/ - Accessed Apr. 2016.

[59] MOE, . Guideline for greenhouse gas emissions reporting. Tech. Rep.; Ontario Ministry of the Environment; 2014.

[60] DOJ, . Electricity and gas inspection regulations - part ix - limits of error. Tech. Rep.; Department of Justice; 2016. http://laws-lois.justice.gc.ca - Accessed Aug. 2016.

[61] IESO, . Realtime constrained totals report. Tech. Rep.; Independent Electricity System Operator; 2013. http://reports.ieso.ca/public/RealtimeConstTotals/ - Accessed Aug. 2016.

[62] Navigant, . Distribution line losses study - prepared for Hydro One Networks Inc. Tech. Rep.; Hydro One; 2014. http://www.hydroone.com - Accessed Aug. 2016.

[63] Wetter, M.. GenOpt generic optimization program - User manual version 3.0.0. Tech. Rep.; Lawrence Berkeley National Laboratory; 2009. http://SimulationResearch.lbl.gov.